

Pre-Processing Matters: Similarity-based Simulated Annealing Approach for Fast Parameter Tuning in WSI Classification

Jun Wang, Yufei Cui, Yu Mao, Nan Guan, Chun Jason Xue,

{jwang699-c, yumao7-c}@my.cityu.edu.hk, yufei.cui@mail.mcgill.ca, nanguan@cityu.edu.hk
jason.xue@mbzuai.ac.ae

Abstract

Pre-processing whole slide images (WSIs) can impact classification performance. Our study shows that using fixed hyper-parameters for pre-processing out-of-domain WSIs can significantly degrade performance. Therefore, it is critical to search domain-specific hyper-parameters during inference. However, searching for an optimal parameter set is time-consuming. To overcome this, we propose SSAPT, a novel Similarity-based Simulated Annealing approach for fast parameter tuning to enhance inference performance on out-of-domain data. The proposed SSAPT achieves 5% to 50% improvement in accuracy with $\times 5$ times faster parameter searching speed on average.

Introduction

Following the success of early CPATH applications, dataset sizes have increased, prompting more multicentric efforts to address variability in staining, image quality, scanning characteristics, and tissue preparation across different labs. This has highlighted a known issue where CPATH algorithms perform best on data they were trained on but less well on data from other sources. Generalization continues to pose a major challenge in this field, as significant differences in clinical variables between tissue source sites can adversely affect the performance of histopathological tasks (Van der Laak, Litjens, and Ciompi 2021; Dehkharhghanian et al. 2023; Howard et al. 2021).

State-of-the-art MIL models have shown promising improvements in WSI classification on out-of-domain data by training on large, diverse datasets (Zhang et al. 2022; Campanella et al. 2019; Lu et al. 2021; Shao et al. 2021; Li, Li, and Eliceiri 2021; Tang et al. 2023). Out-of-domain classification occurs when a model is trained on one dataset and tested on another from a different domain. For instance, a model might be trained using Camelyon16 data (Litjens et al. 2018) and then evaluated using data from various centers in Camelyon17. However, these studies typically only report average accuracy, neglecting the variability in performance across different centers. As indicated in Table 1, the performance of a model trained on Camelyon16 can vary significantly at specific centers within Camelyon17.

We discovered that unsatisfactory performance is often due to using the same inference hyper-parameter across different centers. In real-world scenarios, we apply the

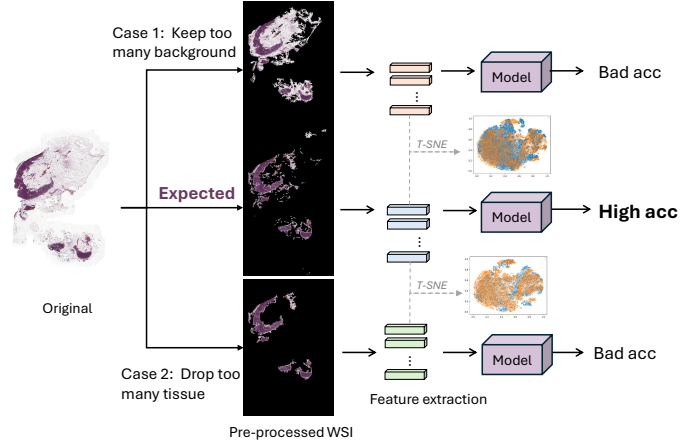


Figure 1: Different pre-processing methods for Whole Slide Images (WSIs) generate distinct features, which in turn affect inference performance. Retaining excessive background and discarding too much tissue can result in poor inference outcomes.

fixed pre-processing parameters to extract features and evaluate performance on new sub-datasets. However, this approach typically results in poor out-of-domain performance (Howard et al. 2021). For example, MIL models (Lu et al. 2021; Cui et al. 2023; Li, Li, and Eliceiri 2021) have extremely low accuracy at specific centers within TCGA and Camelyon17 datasets. Conversely, tailoring optimal pre-processing parameters for each center significantly improves out-of-domain performance (as illustrated in Figure 2).

Determining optimal pre-processing parameters for histopathological tasks is challenging due to the vast size of Whole Slide Images (WSIs) and the significant computational resources needed. Traditional grid search methods for datasets like Camelyon or TCGA are inefficient, taking several hours to evaluate one parameter group. The whole hyper-parameter space contains hundreds of thousands of possible combinations. Therefore, quicker hyper-parameter search techniques are essential for histopathological tasks.

We have observed that varying pre-processing methods can significantly impact model performance during both inference and training. This paper focuses on how

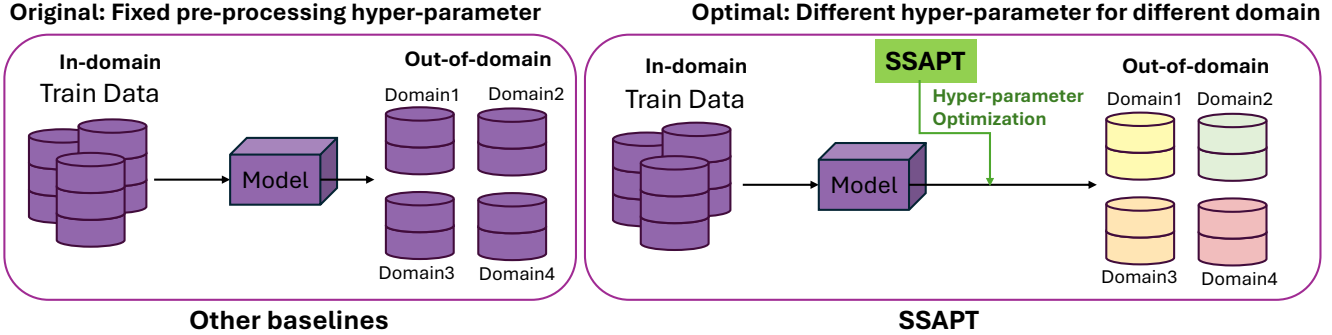


Figure 2: The performance of out-of-domain inference varies with preprocessing parameters across various MIL models and datasets. Consequently, we suggest that each specific center within the dataset should adopt its own preprocessing parameters to maximize performance. The original method involves all centers using fixed default preprocessing hyperparameters, whereas the optimal method allows each center to use its own specific preprocessing hyperparameters determined by our proposed SSAPT.

pre-processing parameters influence inference performance, particularly with out-of-domain data. This paper proposes SSAPT, Similarity-based Simulated Annealing for Hyper-parameter Tuning, a method that improved the accuracy of inferring out-of-domain data by 5% to 50% across various MIL models and datasets. Previous studies, such as those cited in (Choi et al. 2024), only explored hyper-parameter optimization in terms of per-layer learning rates and loss weight coefficients, without tailoring their approaches to histopathology applications. The key contributions of this paper are:

- We have observed that varying pre-processing parameters significantly impact feature extraction and, consequently, model performance—particularly in out-of-domain inference;
- We present SSAPT, Similarity-based Simulated Annealing for fast and effective parameter tuning. This algorithm enhances inference performance at Camelyon 17’s center 1, boosting accuracy from 0.512 to 0.847;
- We expand the proposed SSAPT to include other MIL models using various public datasets, achieving improvements in accuracy ranging from 5% to 50% for out-of-domain data across multiple MIL models and datasets;
- The proposed SSAPT is the first fast hyper-parameter search specifically designed for histopathological tasks.

Related work

MIL models. DSMIL and CLAM employ instance-loss for training, with DSMIL featuring an instance-level classifier. Bayes-MIL focuses on patch-level uncertainty. Trans-MIL (Shao et al. 2021) treats patches as tokens to utilize transformer architecture. MHIM (Tang et al. 2023) employs a masked hard instance mining strategy. All these models are designed at the instance/patch level, which leads to poor out-of-domain performance. In contrast, ABMIL (Ilse, Tomczak, and Welling 2018) operates solely at the bag level, resulting in lower accuracy in in-domain performance across various datasets but achieving greater robustness. However,

it is impossible to completely avoid instance-level design in developing new MIL models for histopathology.

Pre-processing of WSI in histopathology. Variations in tissue processing techniques, including chemical fixation or freezing, dehydration, embedding, and staining, can alter the visual characteristics of the tissue slide in ways that are both non-uniform and non-linear. These changes occur across different tissue types and laboratories (Asif et al. 2023; Yagi 2011), consequently impact the performance in deep learning. Salvi et al.; Gurcan et al. summarize the pre-processing impact for WSI analysis on deep learning frameworks. Tellez et al. quantifies the effects of data augmentation and stain color normalization. (Lee et al. 2022)

There are several research works that specifically explore the issue of dataset bias in CPath. Pocevičiūtė et al. quantifies the impact of domain shift in attention-based MIL and point out that MIL performance is worse than what is reported using in-domain test data. Dehkharghanian et al.; Howard et al. discusses bias on histopathological data. Important clinical variables have been shown to be significantly different between tissue source sites, affecting the generalization issue for histopathological tasks.

Hyper-parameters search and optimization in machine learning. Falkner, Klein, and Hutter propose a Bayesian optimization with Hyperband strategy and evaluate it in small datasets. Choi et al. search hyper-parameters in per-layer learning rates and loss weight coefficients. These previous works are not designed for histopathology.

Motivation and Observation

Public datasets often combine data from various domains (Torralba and Efros 2011; Pocevičiūtė et al. 2023), obscuring true performance metrics within specific areas. Studies (Dehkharghanian et al. 2023; Howard et al. 2021; Hosseini et al. 2024) show that domain-specific variations in digital histology can affect the accuracy and bias of deep learning models. In practice, these variations necessitate frequent retraining of models due to changing data domains, which is impractical due to high computational costs. Thus,

Table 1: **Performance of Out-of-Domain Inference in Specific Challenging Case.** The performance is reported as the average of Accuracy, AUC, Precision, Recall, and F-score metrics, computed over the 10-fold models.

Model	In-Domain (C16)		Out-of-Domain (C17 Center 1)									
	Acc	AUC	Accuracy		AUC		Precision		Recall		F-score	
			Min	Max	Min	Max	Min	Max	Min	Max	Min	Max
ABMIL	0.901	0.941	0.84	0.92	0.833	0.896	0.788	0.966	0.743	0.829	0.765	0.875
DSMIL	0.925	0.954	0.64	0.89	0.721	0.93	0.491	1.000	0.429	0.943	0.556	0.831
CLAM	0.901	0.946	0.512	0.847	0.708	0.833	0.486	0.839	0.743	1.000	0.648	0.788
TransMIL	0.892	0.935	0.73	0.84	0.861	0.914	0.730	0.823	0.753	0.844	0.724	0.830
Bayes-MIL	0.883	0.916	0.35	0.80	0.819	0.881	0.350	0.759	0.629	1.000	0.519	0.737
MHIM-DSMIL	0.925	0.965	0.77	0.87	0.850	0.921	0.607	1.000	0.600	0.971	0.710	0.800

improving model performance without additional training is essential.

Pre-processing Impacts Inference Performance for Different Domains. We found there exists significant variability in inference performance on out-of-domain data across various methods (refer to Table 1). For instance, the CLAM model trained on the Camelyon16 dataset achieves an overall inference accuracy of 0.86 on the Camelyon17 dataset but drops to 0.512 at Center 1 of Camelyon17, indicating inconsistent performance. We have also tested our approach in other centers and datasets, as detailed in the Appendix.

We employ a grid search to fully understand how pre-processing parameters influence outcomes. We discovered that modifying these parameters affects out-of-domain (OOD) inference accuracy differently across centers. The default pre-processing setting yields varying results depending on the center as shown in Fig 3, where identical hyperparameters may perform well in one center but poorly in another. Similar variations are observed across other datasets and MIL models (additional details provided in Appendix). This inconsistency stems from instance/patch-level design choices. We conduct experiments to examine how adjusting bag loss and instance loss weights for DSMIL and CLAM impacts OOD inference performance. Comprehensive details about these instance-level design experiments are available in the Appendix.

Inefficient Manual Pre-Processing Parameter Search. It's beneficial to optimize parameter performance, but finding the best settings is time-consuming; it takes approximately 7 hours to extract features and evaluate a set of parameters on an RTX3080 (details in Appendix). Therefore, we need more efficient parameter search methods. Common strategies like grid search require excessive computational resources and time, rendering them impractical for this scenario.

Based on these observations, we want to explore three questions.

- Can modifying only the preprocessing improve inference performance on out-of-domain data?
- How can we search for parameters more cost-effectively to enhance inference performance?

- Do these observations apply to other state-of-the-art (SOTA) models?

Therefore, we introduce our approach in fast hyperparameter search in pre-processing parameters of histopathology.

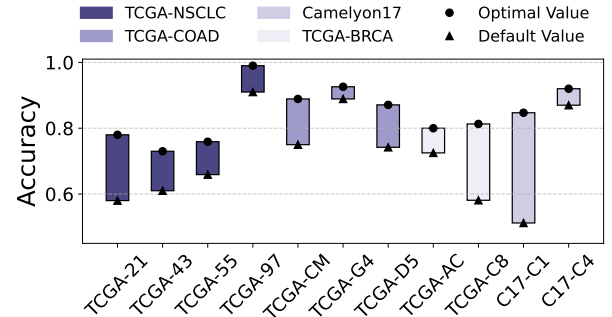


Figure 3: The inference performance of out-of-domain data varies with preprocessing parameters across various MIL models and datasets.

Fast Hyper-Parameter Search for Inference Performance in Out-Of-Domain Data

In this section, we formalize hyperparameter optimization and present our SSAPT algorithm step by step. The proposed SSAPT algorithm includes PSNR-based mechanism for limiting the current searching space in each iteration and Simulated Annealing to avoid local optima.

Definition of Problem

A good choice of hyperparameters can significantly improve out-of-domain inference performance, yet optimal hyperparameters vary, depending on the datasets and the models. Formally, we denote the fast hyper-parameter search algorithm as $H_{opt} = SSAPT(H, D_{val}^n)$ and its hyperparameters as $H \in \Phi$, where Φ is the hyper-parameter space. We denote the training and validation datasets as D_{train} and D_{val} , respectively. The model M is trained in D_{train} , where all WSIs are using fixed hyper-parameter H_{train} . We denote the next inferring processing as $y =$

$\text{Infer}(H_i, D_{\text{val}}^n)$. Hyperparameter optimization finds hyperparameters that maximize some performance metric y . We formalize hyperparameter optimization as

$$H_n^* = \arg \max_{H \in \Phi} \text{Infer}(SSAPT(H, D_{\text{val}}^n), D_{\text{val}}^n) \quad (1)$$

General Assumptions

We assume access to two types of datasets: (1) a large dataset D_{train} for training to produce the foundation model subsequently used to test out-of-domain performance. (2) Multiple subdataset $\{D_{\text{val}} = D_{\text{val}}^1, D_{\text{val}}^2, \dots, D_{\text{val}}^n\}$. The validation sub-dataset D_{val} is much smaller than D_{train} and is used only for optimization at the outer level, not for finetuning. Note that these test distributions are distinct and are never shown to the model before the final evaluation.

Let M denote a pre-trained foundation model trained in a large dataset D_{train} with the pre-processing parameter H_{train} . Note that the model M is trained by k-fold, StratifiedKFold, or Monte Carlo cross-validation, so D_{train} actually contains a sub-dataset of training, validation, and testing while training.

Now, there are many out-of-domain datasets $\{D_{\text{val}} = D_{\text{val}}^1, D_{\text{val}}^2, \dots, D_{\text{val}}^n\}$. They are pre-processed by hyper-parameter H_1, H_2, \dots, H_n to obtain the features $F_{\text{val}}^1, F_{\text{val}}^2, \dots, F_{\text{val}}^n$ for inferring. The out-of-domain performance of model M would be tested by the features F_{val}^n that are preprocessed by the hyper-parameter H_n . We adapt our algorithms as $H_n^* = SSAPT(H_n, D_{\text{val}}^n)$ to search the optimal hyper-parameters H_n for out-of-domain dataset D_{val}^n .

In our experiments, the performance metric y is accuracy, due to the unbalanced datasets in histopathological tasks. For instance, some centers contain only one category of WSI in TCGA-NSCLC, resulting in the situation that AUC and F-score cannot be calculated. Furthermore, extremely low accuracy is reported in some challenging cases, leading to the situation that accuracy is lower than 0.5, but the AUC is still higher than 0.8 (as shown in Table 1).

Pre-Processing Problem Modeling

We define the task of identifying the optimal hyperparameter for enhanced out-of-domain performance as an optimization problem, as described in Equation 1. In practice, this involves repeatedly applying different features within the same foundational model using various hyperparameters H_n^i . This process helps us determine the most effective final hyper-parameters H_n for each validation center D_{val}^n . We assess the effectiveness of each H_n^i by evaluating its performance on the OOD validation set D_{val}^n .

Next we consider the optimization problem for histopathological tasks. The optimization of H_n is actually the optimization of a combination of pre-processing parameters, not a single variable. Previous pre-processing of WSIs encompasses a series of standard procedures. Initially, tissue segmentation is executed automatically on each slide at a reduced magnification. This involves generating a binary mask for the tissue regions by applying a binary

threshold to the saturation channel of the downsampled image, following its conversion from RGB to HSV color space. Morphological closing and median blurring are employed for smoothing the contours of the detected tissue and in minimizing artifacts. Subsequently, the approximate contours of both the tissue and the tissue cavities are assessed and filtered based on their area, culminating in the creation of the final segmentation mask. We complete set of pre-processing hyperparameters for optimization in histopathological tasks is thus $H_n = [x_1, x_2, x_3, x_4, x_5, x_6]$, where each x_i has its own hyper-parameter space.

Optimization of Fast Hyper-Parameter Search

Good Pre-Processed WSIs show High Structural Similarity. For single-domain inference performance, our experiments demonstrate that pre-processing parameters yielding accurate predictions produce images with similar structures (as illustrated in Figure 5). Therefore, we only evaluate the pre-processed Whole Slide Images (WSIs) that closely resemble the optimally pre-processed WSI. To quantitatively assess differences between two sets of pre-processing results, we use Peak Signal-to-Noise Ratio (PSNR) to measure the similarity of images generated during patch creation. As depicted in Figure 1, our workflow includes creating patches, extracting features, training models, and testing inference data. During patch generation, thumbnails are created for visualizing the preprocessing effects. Thus, we can determine the similarity between these two sets of pre-processed results by calculating PSNR for these thumbnails.

PSNR Peak Signal-to-Noise Ratio (PSNR) is a common measurement in image processing and digital signal processing. A higher PSNR value indicates greater similarity between two images. We calculate the PSNR by comparing thumbnails generated during preprocessing. For example, the total PSNR of thumbnails produced using the second-best preprocessing parameters should be higher than that of any other set, as illustrated in Figure 5.

$$\text{PSNR} = 10 \cdot \log_{10} \left(\frac{\text{MAX}^2}{\frac{1}{N} \sum_{i=1}^N (I_i - K_i)^2} \right). \quad (2)$$

In our motivation experiments, which explore the impact of pre-processing parameters on out-of-domain performance, we have already processed sufficient Whole Slide Images (WSIs) with inference results. We established the similarity threshold τ based on previous experimental analyses. For our proposed SSAPT method, we use H_{train} as the default parameter. Using the current optimal parameter H^* , we generate a new parameter H_{new} , create patches, and calculate their PSNR against the optimal thumbnails I^* . If the PSNR exceeds threshold τ , we proceed to more resource-intensive tasks such as feature extraction in histopathological analysis and subsequent inference using an existing model. Each new parameter set H_{new} is added to our historical dataset $R = \{(H_1, y_1), \dots, (H_i, y_i)\}$. If H_{new} demonstrates improved performance, there is a probability p (as per Eq.(3)) that H^* will be updated with H_{new} . This process will be further discussed in the following subsection.

Algorithm 1: Similarity based Simulated Annealing for Parameter Tuning (SSAPT)

Input: Default parameter H_{train} with result set \mathcal{R} , Hyper-parameters space Φ , initial temperature T_0 , minimum temperature T_{min} , cooling rate α , similarity threshold τ , function $Infer$ to evaluate performance, function S to calculate similarity, p is the acceptance probability function

Output: Optimal parameters H^*

```

1: Initialize  $H^*$  with fixed default parameter  $H_{train}$ 
2: Generate pre-processed thumbnail  $I^*$  from  $H^*$ 
3: Generate feature  $F^*$  from WSIs with  $H^*$ 
4:  $y^* \leftarrow Infer(F^*)$ 
5:  $\mathcal{R} \leftarrow (H^*, y^*)$ 
6:  $T \leftarrow T_0$ 
7: while  $T > T_{min}$  do
8:   Select  $H_{new}$  by perturbing  $H^*$  slightly from  $\Phi$ 
9:   if  $H_{new}$  not in  $\mathcal{R}$  then
10:    Generate thumbnail  $I_{new}$  with  $H_{new}$ 
11:     $\Delta s \leftarrow S(I_{new}, I^*) - \tau$ 
12:    if  $\Delta s > 0$  then
13:      Extract feature  $F_{new}$        $\triangleright$  Expensive step
14:       $y_{new} \leftarrow Infer(F_{new})$ 
15:       $\mathcal{R} \leftarrow \mathcal{R} \cup (H_{new}, y_{new})$ 
16:      if  $y_{new} > y^*$  then
17:         $H^*, I^*, y^* \leftarrow H_{new}, I_{new}, y_{new}$  with  $p$ 
18:      end if
19:    end if
20:     $T \leftarrow \alpha T$ 
21:  end if
22: end while
23: return  $H^*$ 

```

Similarity-based Simulated Annealing for Parameter Tuning

To avoid falling into local optima, we integrate the Simulated Annealing algorithm (Kirkpatrick, Gelatt Jr, and Vecchi 1983) into our method to identify optimal parameters. We detail SSAPT in Algorithm 1. Our experimental results indicate that creating patches with thumbnails and bypassing most parameter feature extraction processes allows us to refine pre-processing parameters for enhanced inferential performance.

Our algorithm is designed to optimize pre-processing parameters effectively, ensuring high performance while accelerating the overall process. The Simulated Annealing algorithm prevents convergence at local optima by exploring multiple random states near the current solution, akin to simulated annealing itself. Occasionally, we enhance solutions by leveraging the current temperature to explore nearby states post-annealing. This approach introduces randomness through annealing rules, significantly increasing the likelihood of achieving an optimal solution tailored for histopathological tasks.

During each iteration, we aim to match the pre-processed results closely with the current optimum. We use a similarity threshold τ , related to PSNR as a filter mechanism. After patch creation, features are extracted and analyzed only from pre-processed Whole Slide Images (WSIs) that exhibit

a PSNR higher than τ . WSIs with lower PSNR compared to the optimal pre-processed WSI are excluded from further processing. If superior inference performance emerges, updates are made for H^*, I^*, y^* based on acceptance probability p :

$$p(\Delta s) = \exp(\Delta s/T) \quad (3)$$

Experiments

Experiments Setup

Our experiment utilizes the pre-processing pipeline from CLAM. The datasets employed in this study include Camelyon 16, Camelyon 17 (Litjens et al. 2018), TCGA-NSCLC, TCGA-BRCA, and TCGA-COAD (Weinstein et al. 2013). For Camelyon16 and Camelyon17, we focus on normal-tumor classification; for all TCGA datasets, we address subtype tasks.

In our experiments, we standardize seeds and model hyperparameters such as learning rate and loss weight across similar tasks within the same model framework. Additional experimental details are provided in the Appendix. We employ K-fold, StratifiedKFold or k-fold Monte Carlo cross-validation methods (with k set to 10) to train models and assess out-of-domain performance. All results presented in Table 2 and Table 3 represent average accuracies calculated over these 10-fold models.

Classification Accuracy Validation of SSAPT

For the Camelyon datasets, we trained our model using 270 whole slide images (WSIs) from Camelyon16 and tested inference performance across various centers in Camelyon17 to simulate out-of-domain scenarios. It's important to note that Camelyon16 data was collected from UMCU and RUMC, while Camelyon17 includes data from CWZ, RST, UMCU, RUMC, and LPON. Consequently, only centers 0 (CWZ), 1 (RST), and 4 (LPON) of Camelyon17 represent out-of-domain situations.

We compared the inference performance using features extracted by default parameters (not the worst) and those

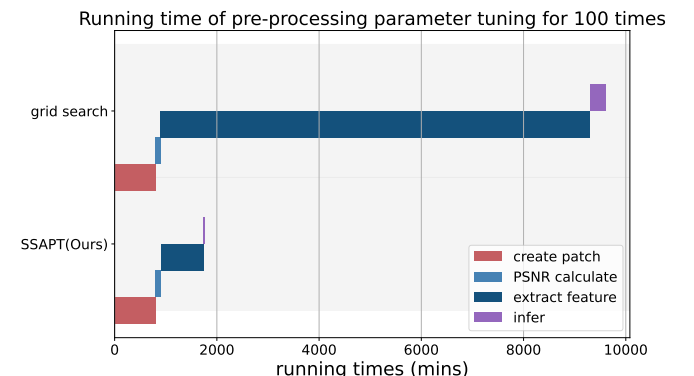


Figure 4: **The running time** of pre-processing parameters tuning for 100 times. Our algorithm can save time by skipping a large number of feature extraction.

Dataset	Center	ABMIL		DSMIL		CLAM		Bayes-MIL		MHIM-DSMIL	
		Default	Ours	Default	Ours	Default	Ours	Default	Ours	Default	Ours
Camelyon17	C0	0.93	0.97	0.77	0.96	0.921	0.95	0.83	0.94	0.87	0.96
	C1	0.87	0.92	0.85	0.89	0.512	0.846	0.35	0.8	0.81	0.87
	C4	0.88	0.93	0.92	0.96	0.874	0.92	0.85	0.92	0.91	0.94
TCGA-COAD	CM	0.75	0.778	0.75	0.778	0.75	0.889	0.861	0.889	0.75	0.801
	D5	0.709	0.774	0.806	0.871	0.742	0.871	0.709	0.806	0.839	0.871
	DM	0.783	0.826	0.869	0.869	0.739	0.739	0.783	0.826	0.826	0.87
	G4	0.963	0.963	0.963	0.963	0.889	0.926	0.926	1	0.925	0.963
TCGA-BRCA	A7	0.902	0.961	0.921	0.941	0.941	0.961	0.882	0.882	0.923	0.961
	AC	0.775	0.8	0.725	0.8	0.75	0.8	0.775	0.775	0.75	0.775
	AR	0.781	0.8	0.765	0.781	0.813	0.828	0.813	0.828	0.75	0.766
	C8	0.907	0.93	0.581	0.813	0.907	0.93	0.86	0.884	0.907	0.93

Table 2: **Experiments in out-of-domain inference performance.** We compare the accuracy obtained by default hyper-parameters with the optimal hyper-parameter searched by our SSAPT algorithm.

optimized through our SSAPT algorithm. As shown in Table 2, the optimal hyper-parameters identified by our SSAPT algorithm generally surpass the default settings across various models and datasets. In specific cases, such as with CLAM and BayesMIL at Center 1, performance improved dramatically from below 0.5 to up to 0.8 simply by adjusting the hyper-parameters. Even for robust models like ABMIL, modifying parameters proved effective.

For TCGA datasets, we divide the entire dataset according to TCGA Tissue Source Site Codes. We select several centers with a sufficient number of WSIs to form the testing sub-dataset, while the remaining data constitutes the training dataset. The out-of-domain inference performance also improves (as shown in Table 2), indicating that our issue is general and our SSAPT provides a universal solution. Additionally, we conduct experiments on a larger TCGA-NSCLC dataset that includes more extensive out-of-domain testing (as detailed in Table 3).

Dataset	Center	ABMIL		CLAM		Bayes-MIL	
		Def.	Ours	Def.	Ours	Def.	Ours
TCGA-NSCLC	21	0.722	0.778	0.556	0.778	0.556	0.667
	22	0.865	0.892	0.784	0.838	0.838	0.838
	43	0.750	0.800	0.600	0.750	0.700	0.800
	49	0.595	0.643	0.690	0.714	0.714	0.762
	55	0.495	0.516	0.659	0.758	0.275	0.330
	77	0.932	0.932	0.909	0.932	0.750	0.800
	97	1.000	1.000	0.913	1.000	0.869	0.957

Table 3: Comparison of inference accuracy in TCGA-NSCLC. We evaluate the default hyper-parameter with optimal hyper-parameter searched by our SSAPT Algorithm in a larger dataset TCGA-NSCLC with more centers.

Efficiency Validation

Figure 4 shows the running time for tuning preprocessing parameters 100 times. Our Simulated Annealing algorithm for Parameter Tuning uses PSNR to compare each pre-processed WSI with the best one so far, selecting only those

with high similarity for further feature extraction. WSIs with low PSNR are skipped, streamlining the process and ensuring that only promising candidates are evaluated further. This approach prevents our SSAPT from getting stuck in local optima and saves time by reducing unnecessary feature extractions.

Ablation Study

PSNR Without the PSNR-based strategy, the algorithm performs a random search. It randomly generates pre-processing parameters, creates patches, extracts features, and assesses performance in each iteration without skipping feature extraction (as shown in Table 4).

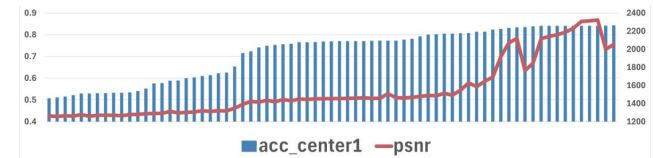


Figure 5: **The evidence of PSNR-based mechanism** works in our fast hyper-parameter search in histopathological tasks.

We also assess FDD-Simulated Annealing. It's important to note that the Fréchet domain distance (FDD) in this part of the ablation study serves a different role compared to its use in the Discussion section. Here, FDD replaces PSNR for comparison purposes. Both FDD and PSNR-based mechanisms in this ablation study are employed to constrain the search space for optimal hyper-parameters, rather than searching across the entire hyper-parameter space.

Simulated Annealing Simulated Annealing prevents optimization from getting stuck in local optima. As illustrated in Table 5, search algorithms lacking Simulated Annealing repeatedly test hyper-parameters that yield a higher PSNR than the current optimal solution.

Table 4: **Importance of the PSNR.** Results are based on optimizing 100 times in the center1 of Camelyon17. SA stands for Simulated Annealing, Lat. stands for Latency and Mem. stands for Memory.

Strategy	Acc	Lat. (min)	Mem. (GB)
None (Baseline)	0.847	9600	1250
FDD-SA	0.846	5350	650
PSNR-SA (Ours)	0.846	1770	170

Table 5: **Importance of Simulated Annealing (SA).** Results based on optimizing 100 times in center1 of Camelyon17.

Strategy	Accuracy	Latency (min)
Without SA	0.829	4119
With SA	0.846	1770

Discussion

Quantifying the Initial Features

We demonstrate that significant differences exist in the initial features extracted by various pre-processing parameters, which are used as inputs for training models or making inferences. These differences arise not only from distribution shifts but also from variations in the number of patches extracted from each WSI, leading to partial information loss. For the same WSI, we compare features generated under different hyper-parameter settings: H_{opt} , H_{good} , and H_{random} . As shown in Figures 1 and 6, features are similar when their inference performance is comparable. However, Figure 6 (Right) highlights distinct differences between H_{opt} and H_{random} within the t-SNE space, underscoring how patch count variations can exacerbate feature representation discrepancies and affect out-of-distribution (OOD) inference performance.

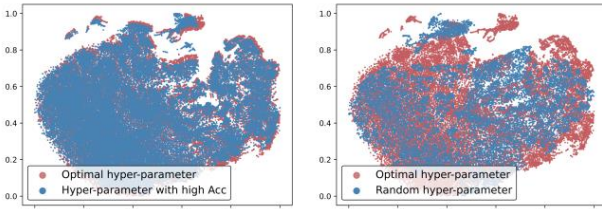


Figure 6: **The visualization of comparison between features.** **Left:** The comparison of the feature obtaining high accuracy with the optimal feature. **Right:** The comparison of the feature extracted by random hyper-parameters with the optimal one. Note that these features are extracted from the same WSIs.

Evaluating the Influence of Pre-processing on Model Representations We utilize Fréchet domain distance (FDD) (Pocevičiūtė et al. 2023) to compare features from the penultimate layer and assess how pre-processing parameters influence the model’s representations. For each spe-

cific out-of-domain testing dataset D_{val}^i , WSIs undergo pre-processing using H_i to generate feature F_i . This feature is then input into the model for inference. We extract the penultimate layer feature P_i before it reaches the final classifier. The same process applies when using optimal pre-processing features identified by our SSAPT algorithm, denoted as H_{opt} , resulting in F_{opt} . For WSIs processed with H_i , a higher accuracy correlates with a lower FDD compared to those processed with optimal pre-processing (H_{opt}), as illustrated in Figure 7.

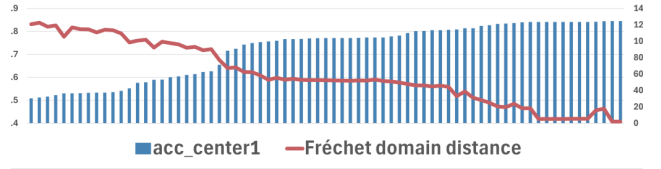


Figure 7: Quantifying the Features Impact by Model Visibility.

SSAPT is designed for histopathological tasks

Previous hyper-parameter optimization strategies (Falkner, Klein, and Hutter 2018; Choi et al. 2024) have been developed with a focus on general machine learning models and evaluated on datasets characterized by a large number of images but relatively small image sizes. However, the unique characteristics of WSIs should not be ignored. WSIs are giga-pixel images that demand significantly higher computational resources. Despite advancements in hardware, memory constraints still pose a significant challenge in the digital processing of WSIs in current research (Cifci et al. 2023; Echle et al. 2021). Additionally, nature images have very different data distribution compared to the whole slide image (Raghu et al. 2019). Therefore, designing hyper-parameter optimization strategy for CPath is necessary. The proposed SSAPT algorithm is the first hyper-parameter optimization strategy designed for histopathological tasks.

Conclusion

Different pre-processing parameters significantly impact feature extraction and model performance in histopathological tasks. In this paper, we propose the Similarity-based Simulated Annealing (SSAPT) algorithm for fast parameter tuning, which enhances inference performance on out-of-domain data. SSAPT achieves a 5% to 50% accuracy improvement on the Camelyon and multiple TCGA datasets, offering faster hyper-parameter search by reducing feature extraction steps based on WSI characteristics.

References

Asif, A.; Rajpoot, K.; Graham, S.; Snead, D.; Minhas, F.; and Rajpoot, N. 2023. Unleashing the potential of AI for pathology: challenges and recommendations. *The Journal of Pathology*, 260(5): 564–577.
 Campanella, G.; Hanna, M. G.; Geneslaw, L.; Miraflor, A.; Werneck Krauss Silva, V.; Busam, K. J.; Brogi, E.; Reuter,

V. E.; Klimstra, D. S.; and Fuchs, T. J. 2019. Clinical-grade computational pathology using weakly supervised deep learning on whole slide images. *Nature medicine*, 25(8): 1301–1309.

Choi, C.; Lee, Y.; Chen, A.; Zhou, A.; Raghunathan, A.; and Finn, C. 2024. AutoFT: Robust Fine-Tuning by Optimizing Hyperparameters on OOD Data. *arXiv preprint arXiv:2401.10220*.

Cifci, D.; Veldhuizen, G. P.; Foersch, S.; and Kather, J. N. 2023. AI in computational pathology of cancer: improving diagnostic workflows and clinical outcomes? *Annual Review of Cancer Biology*, 7(1): 57–71.

Cui, Y.; Liu, Z.; Liu, X.; Liu, X.; Wang, C.; Kuo, T.-W.; Xue, C. J.; and Chan, A. B. 2023. Bayes-MIL: A new probabilistic perspective on attention-based multiple instance learning for whole slide images. In *11th International Conference on Learning Representations (ICLR 2023)*.

Dehkharghanian, T.; Bidgoli, A. A.; Riasatian, A.; Mazaheri, P.; Campbell, C. J.; Pantanowitz, L.; Tizhoosh, H.; and Rahnamayan, S. 2023. Biased data, biased AI: deep networks predict the acquisition site of TCGA images. *Diagnostic pathology*, 18(1): 67.

Echle, A.; Rindtorff, N. T.; Brinker, T. J.; Luedde, T.; Pearson, A. T.; and Kather, J. N. 2021. Deep learning in cancer pathology: a new generation of clinical biomarkers. *British journal of cancer*, 124(4): 686–696.

Falkner, S.; Klein, A.; and Hutter, F. 2018. BOHB: Robust and efficient hyperparameter optimization at scale. In *International conference on machine learning*, 1437–1446. PMLR.

Gurcan, M. N.; Boucheron, L. E.; Can, A.; Madabhushi, A.; Rajpoot, N. M.; and Yener, B. 2009. Histopathological image analysis: A review. *IEEE reviews in biomedical engineering*, 2: 147–171.

Hosseini, M. S.; Bejnordi, B. E.; Trinh, V. Q.-H.; Chan, L.; Hasan, D.; Li, X.; Yang, S.; Kim, T.; Zhang, H.; Wu, T.; et al. 2024. Computational pathology: a survey review and the way forward. *Journal of Pathology Informatics*, 100357.

Howard, F. M.; Dolezal, J.; Kochanny, S.; Schulte, J.; Chen, H.; Heij, L.; Huo, D.; Nanda, R.; Olopade, O. I.; Kather, J. N.; et al. 2021. The impact of site-specific digital histology signatures on deep learning model accuracy and bias. *Nature communications*, 12(1): 4423.

Ilse, M.; Tomczak, J.; and Welling, M. 2018. Attention-based deep multiple instance learning. In *International conference on machine learning*, 2127–2136. PMLR.

Kirkpatrick, S.; Gelatt Jr, C. D.; and Vecchi, M. P. 1983. Optimization by simulated annealing. *science*, 220(4598): 671–680.

Lee, Y.; Park, J. H.; Oh, S.; Shin, K.; Sun, J.; Jung, M.; Lee, C.; Kim, H.; Chung, J.-H.; Moon, K. C.; et al. 2022. Derivation of prognostic contextual histopathological features from whole-slide images of tumours via graph deep learning. *Nature Biomedical Engineering*, 1–15.

Li, B.; Li, Y.; and Eliceiri, K. W. 2021. Dual-stream multiple instance learning network for whole slide image classification with self-supervised contrastive learning. In *Proceedings of the IEEE/CVF conference on computer vision and pattern recognition*, 14318–14328.

Litjens, G.; Bandi, P.; Ehteshami Bejnordi, B.; Geessink, O.; Balkenhol, M.; Bult, P.; Halilovic, A.; Hermsen, M.; van de Loo, R.; Vogels, R.; et al. 2018. 1399 H&E-stained sentinel lymph node sections of breast cancer patients: the CAMELYON dataset. *GigaScience*, 7(6): giy065.

Lu, M. Y.; Williamson, D. F.; Chen, T. Y.; Chen, R. J.; Barbieri, M.; and Mahmood, F. 2021. Data-efficient and weakly supervised computational pathology on whole-slide images. *Nature biomedical engineering*, 5(6): 555–570.

Pocevičiūtė, M.; Eilertsen, G.; Garvin, S.; and Lundström, C. 2023. Detecting Domain Shift in Multiple Instance Learning for Digital Pathology Using Fréchet Domain Distance. In *International Conference on Medical Image Computing and Computer-Assisted Intervention*, 157–167. Springer.

Raghu, M.; Zhang, C.; Kleinberg, J.; and Bengio, S. 2019. Transfusion: Understanding transfer learning for medical imaging. *Advances in neural information processing systems*, 32.

Salvi, M.; Acharya, U. R.; Molinari, F.; and Meiburger, K. M. 2021. The impact of pre-and post-image processing techniques on deep learning frameworks: A comprehensive review for digital pathology image analysis. *Computers in Biology and Medicine*, 128: 104129.

Shao, Z.; Bian, H.; Chen, Y.; Wang, Y.; Zhang, J.; Ji, X.; et al. 2021. Transmil: Transformer based correlated multiple instance learning for whole slide image classification. *Advances in neural information processing systems*, 34: 2136–2147.

Tang, W.; Huang, S.; Zhang, X.; Zhou, F.; Zhang, Y.; and Liu, B. 2023. Multiple instance learning framework with masked hard instance mining for whole slide image classification. In *Proceedings of the IEEE/CVF International Conference on Computer Vision*, 4078–4087.

Tellez, D.; Litjens, G.; Bárdi, P.; Bulten, W.; Bokhorst, J.-M.; Ciompi, F.; and Van Der Laak, J. 2019. Quantifying the effects of data augmentation and stain color normalization in convolutional neural networks for computational pathology. *Medical image analysis*, 58: 101544.

Torralba, A.; and Efros, A. A. 2011. Unbiased look at dataset bias. In *CVPR 2011*, 1521–1528. IEEE.

Van der Laak, J.; Litjens, G.; and Ciompi, F. 2021. Deep learning in histopathology: the path to the clinic. *Nature medicine*, 27(5): 775–784.

Weinstein, J. N.; Collisson, E. A.; Mills, G. B.; Shaw, K. R.; Ozenberger, B. A.; Ellrott, K.; Shmulevich, I.; Sander, C.; and Stuart, J. M. 2013. The cancer genome atlas pan-cancer analysis project. *Nature genetics*, 45(10): 1113–1120.

Yagi, Y. 2011. Color standardization and optimization in whole slide imaging. In *Diagnostic pathology*, volume 6, 1–12. Springer.

Zhang, H.; Meng, Y.; Zhao, Y.; Qiao, Y.; Yang, X.; Coupland, S. E.; and Zheng, Y. 2022. DTFD-MIL: Double-tier feature distillation multiple instance learning for histopathology whole slide image classification. In *Proceedings of the IEEE/CVF Conference on Computer Vision and Pattern Recognition*, 18802–18812.